available at www.sciencedirect.com

SCIENCE DIRECT®

journal homepage: www.elsevier.com/locate/biochempharm

Preclinical analysis of the analinoquinazoline AG1478, a specific small molecule inhibitor of EGF receptor tyrosine kinase

A.G. Ellis [a,1], M.M. Doherty [b,1], F. Walker [c], J. Weinstock [c], M. Nerrie [c], A. Vitali [c], R. Murphy [c], T.G. Johns [c], A.M. Scott [c], A. Levitzki [d], G. McLachlan [e], L.K. Webster [a], A.W. Burgess [c], E.C. Nice [c,*]

[a] Pharmacology and Developmental Therapeutics Unit, Trescowthick Research Laboratories, Peter MacCallum Cancer Centre, Melbourne, Vic., Australia
[b] Department of Pharmaceutics, Victorian College of Pharmacy, Monash University, Melbourne, Vic., Australia
[c] Ludwig Institute for Cancer Research, Melbourne, Vic., Australia
[d] Department of Biological Chemistry, Alexander Silberman Institute of Life Sciences, Hebrew University of Jerusalem, Jerusalem, Israel
[e] Institute of Drug Technology, Melbourne, Australia

ARTICLE INFO

Article history:
Received 27 November 2005
Accepted 30 January 2006

Keywords:
EGFR receptor
AG1478
Pharmacokinetics
Tyrosine kinase inhibitor
Microphysiometer
Quinazoline

ABSTRACT

The tyrphostin 4-(3-chloroanilino)-6,7-dimethoxyquinazoline (AG1478) is a potent and specific inhibitor of EGFR tyrosine kinase whose favourable preclinical profile supports progression towards clinical trials. Microphysiometric evaluation revealed a short (<24 min) effective inhibition of cellular receptor response to EGF challenge in BaF/ERX cells indicating a need to maintain sustained levels of inhibitor. Initial pharmacokinetic evaluation in mice of novel AG1478 formulations in a beta-cyclodextrin (Captisol®) showed monoexponential elimination from plasma (half-life 30 min) following subcutaneous administration. A two-fold dose escalation gave a 2.4-fold increase in the total AUC. Bolus i.v. and 6 h continuous infusion were investigated in rats to mimic a more clinically relevant administration regimen. Drug elimination following bolus i.v. administration was biphasic (terminal elimination half-life 30–48 min). The linear relationship between dose and $AUC_{0\rightarrow\infty}$ ($r^2 = 0.979$) enabled the prediction of infusion rates and doses for sustained delivery using continuous 6 h infusions, where steady state was reached in 120 min. Plasma levels of AG1478 >10 μM were achieved over the duration of the infusion. At the lowest dose, plasma drug levels after the cessation of infusion declined with a half-life of approximately 43 min. EGFR activity, measured both by autophosphorylation and downstream signalling, was inhibited in a dose-dependent manner by injection of AG1478 in mice bearing xenografts of the human glioblastoma cell line U87MG.Δ2-7, which expresses a constitutively active variant of the EGF receptor. Taken together, these experiments provide essential data to assess the anti-tumour efficacy of AG1478 and will assist in the rational design of dose regimens for clinical studies.

* *Corresponding author at*: Ludwig Institute for Cancer Research, PO Box 2008 RMH, Melbourne, Vic. 3050, Australia. Tel.: +61 3 9341 3155; fax: +61 3 9341 3104.
E-mail address: Ed.Nice@ludwig.edu.au (E.C. Nice).

[1] Authors made equivalent contributions.

0006-2952/$ – see front matter © 2006 Elsevier Inc. All rights reserved.
doi:10.1016/j.bcp.2006.01.020

1. Introduction

The EGFR family (EGFR (erbB1), erbB2 (HER2) erbB3 and erbB4) are a family of receptors that regulate a wide range of cellular processes including proliferation, differentiation, motility, survival, angiogenesis and invasion [1–3]. Increased, or constitutive EGFR signalling due to mutations of the receptor, gene amplification, receptor over-expression or autocrine stimulation by specific ligands has been observed in approximately one third of all human tumours including brain, head and neck, colon, lung and pancreas [3,4]. Such aberrant signalling is often associated with poor clinical prognosis including non-responsiveness to chemotherapy and decreased survival [5]. The EGFR family therefore represents an important target for pharmacological intervention using specific potent inhibitors of these signalling pathways [6].

This has led to the design of a range of inhibitors that target discreet regions of the receptor. Various inhibitors are directed towards the extracellular binding or dimerisation domains and include monoclonal antibodies [7,8], immunotoxins [9,10] and ligand-binding cytotoxic agents [11,12]. However, the group termed 'small molecule inhibitors' target the intracellular tyrosine kinase region, and interfere with the signalling pathways that modulate the cancer-promoting response (see [6,12,13] for reviews).

While there are many classes of small molecule tyrosine kinase inhibitors [14], the quinazolines appear to be among the most promising and the most advanced in clinical development. Clinical trials of two orally administered small molecule reversible inhibitors of ErBb1: gefitinib (ZD1839 or Iressa®, Astra Zeneca) for non-small cell lung cancer, and erlotinib (OSI774 or Tarceva®, OSI Pharmaceuticals) for breast, pancreatic and non-small cell lung cancer have demonstrated significant activity, leading to the former being approved for use in this indication [6,12,15–20]. Other inhibitors also in clinical trial include EKB569 (Wyeth-Ayerst) and CI1033 (Pfizer) however these agents irreversibly inhibit ErbB1 and in the case of CI1033 inhibit all ErbB receptors [12,15,17,18]. The utility of irreversible over reversible inhibitors is yet to be substantiated [21].

There is also mounting evidence to suggest that EGFR tyrosine kinase inhibitors will have synergistic effects with other anti-tumour treatments [22–24] especially in the setting of combined radiation and chemotherapy [25,26]. However, randomised Phase III trials of gefitinib in combination with chemotherapy regimens have shown no survival advantage over the use of chemotherapy alone [27]. An association of response to EGFR kinase inhibitors with mutation status of the tyrosine kinase domain [28,29] has been reported and is the subject of ongoing research.

The tyrphostin (tyrosine phosphorylation inhibitor) 4-(3-chloroanilino)-6,7-dimethoxyquinazoline (AG1478, Fig. 1) [30], which is a competitive inhibitor of the ATP binding site in the kinase domain [31,32] is a highly potent and specific small molecule inhibitor of EGFR (ErbB1) tyrosine kinase [15,33]. The important chemical features for activity against EGFR include: the presence of electron-donating groups at positions 6 and 7 on the quinazoline; the presence of small lipophilic groups at position 3 of the aniline; the orientation of the quinazoline ring nitrogens [14]. The chemical structures of the orally active quinazoline compounds currently in clinical trial differ to AG1478 due to the presence of hydrophilic side chains at positions 6 and/or 7 [14] (Fig. 1).

AG1478 is active both in vitro in cell lines such as colon cancer, non-small cell lung cancer and glioblastoma cell models and in vivo in mice xenograft models. In cell culture experiments it has significant anti-proliferative effects [32–36], and enhances the sensitivity to cytotoxic drugs like cisplatin and doxorubicin [37,38]. In tumour xenograft models AG1478 inhibits the growth of A431 tumours [39] and human glioblastomas [23,24,40] which over-express a mutant EGFR (Δ2-7 EGFR) [41]. AG1478 also sensitises these tumours to the

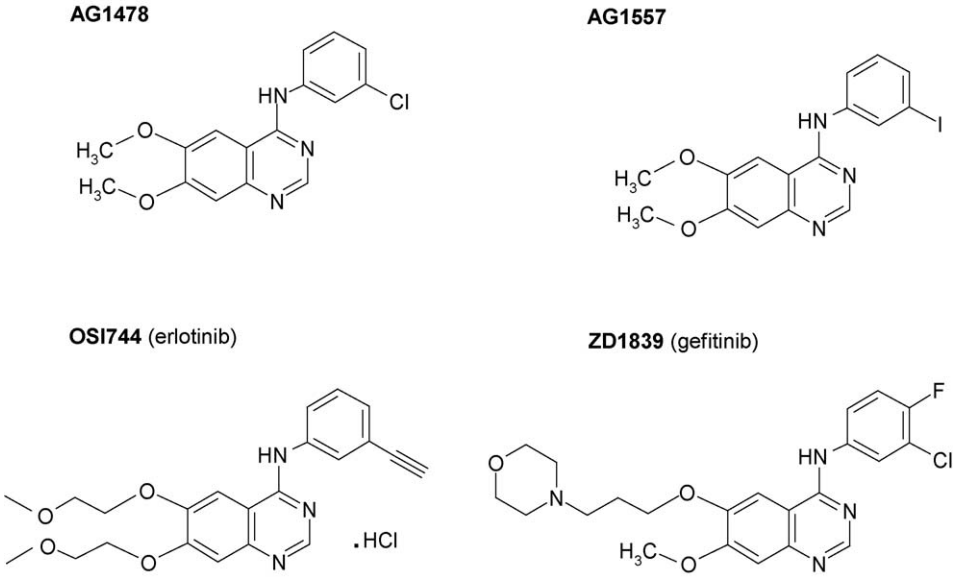

Fig. 1 – The structure of AG1478 (4-(3-chloroanilino)-6,7-dimethoxyquinazoline), AG1557 (4-(3-iodoanilino)-6,7-dimethoxyquinazoline), OSI744 (erlotonib) (*N*-(3-ethynylphenyl)-6,7-bis(2-methoxyethoxy)-4-quinazolinamine·HCl) and ZD1839 (gefitinib) (4-(3-chloro-4-flurophenylamine)-7-methoxy-6(3-(4-morpholinyl)quinazoline)).

cytotoxic action of cisplatin [23] and temozolomide or the monoclonal antibody mAb 806, an anti-EGFR antibody that was raised against the Δ2-7 EGFR but unexpectedly also binds a subset of the EGFR expressed in cells exhibiting amplification of the EGFR gene [24,40].

In this study different salts forms of AG1478 have been combined with sulfo-butylether beta-cyclodextrin (Captisol®, CyDex Inc., Lenexa, KS, USA), which has demonstrated efficacy in improving the aqueous solubility of hydrophobic drugs [42–45]. The Captisol® has permitted aqueous formulations of appropriately high AG1478 concentration (>90 mM) for the assessment of tissue distribution and pharmacokinetics of AG1478 in mice and rats. Mice were used to assess distribution, initial pharmacokinetics and the feasibility of the various formulations and administration routes (subcutaneous and oral). Use of the rat model allowed the determination of individual plasma profiles through multiple blood sampling. Steady state infusion studies, where drug levels could be maintained at predetermined levels, were chosen for the initial determination of pharmacodynamic endpoints. These experiments provide essential data for the design of future experiments to assess the anti-tumour efficacy of AG1478 and will assist in the rational design of dose regimens for the clinical studies.

2. Methods

2.1. Chemicals/reagents

AG1478 (4-(3-chloroanilino)-6,7-dimethoxyquinazoline) as the free base, the chloride, tartrate, citrate or mesylate salts and the internal standard AG1557 (4-(3-iodoanilino)-6,7-dimethoxyquinazoline, Fig. 1) [30], used in the HPLC monitoring, were synthesised by IDT (Institute of Drug Technology, Boronia, Australia). ^{3}H-AG1478 (4.4 Ci/mmol) was prepared by Amersham Biosciences (Cardiff, Wales) and ^{99m}Tc-labelled human serum albumin (^{99m}Tc-HSA) was generated on site (Radiopharmacy Department, Peter MacCallum Cancer Centre, Melbourne, Australia) from commercially available Albumex^{20} (CSL, Parkville, Vic., Australia) with a specific activity of 0.5 mCi/mg (17 Ci/mmol). Captisol® (sulfo-butylether beta-cyclodextrin) was purchased from CyDex Inc. (Lenexa, KS, USA). Dimethylsulfoxide (DMSO), analytical reagent was purchased from Sigma–Aldrich (Castle Hill, NSW, Australia).

2.2. Formulations

2.2.1. Solubility studies

Solubilities were calculated by preparing saturated solutions of the drug in the appropriate buffer. This was achieved by sonication using a sonifier (Branson Consonic, Danbury, USA) (output 5, cycle 50% for 1 min), and then leaving the sample overnight at 25 °C. Samples were then centrifuged for 10 min at 10,000 × *g* and the soluble supernatant carefully removed. The absorbance at 330 nm was read using a spectrophotometer (Carey 50, Varian, Australia) and compared with a standard curve prepared by serial dilutions of AG1478 free base dissolved in DMSO and quantitated using an extinction coefficient at 330 nm of 13,231 mol^{-1} cm^{-1}.

2.2.2. Formulation for animal studies

(a) *Mouse studies*. In initial experiments formulations of either AG1478 tartrate or citrate salts dissolved in water at concentrations well below the maximum solubility were used. Higher concentrations of AG1478 were achieved using Captisol®-containing solutions and were used to deliver doses listed in Table 2. To make these solutions Captisol® was dissolved with stirring in 5% glucose solution, after which the AG1478 salt was added to the solution (0.5 molar ratio to Captisol®) and stirring continued until complete dissolution. For all formulations the final solution of AG1478 mesylate/Captisol® was filtered under aseptic conditions using a Fluorodyne II filter cartridge (Pall Corporation), and dispensed in 5 ml aliquots into 10 ml type II soda glass vials (Kimble Kontes, Vineland, NJ, USA). The vials were sealed with Fluorotec stoppers and aluminium crimp seals (West Pharmaceutical Services, Brookvale, Australia) and stored at 2–8 °C. The identity of AG1478 in the vial contents was confirmed by RP-HPLC analysis and mass spectral analysis, and the concentration confirmed spectrophotometrically at 330 nm prior to administration. Biological activity was determined using the mitogenic assays described below.

(b) *Rat studies*. AG1478 mesylate (49 mM) in Captisol® (98 mM) was prepared as described above.

2.3. Mitogenic assays

Mitogenic assays were performed using the EGF-dependent BaF/ERX [46] and LIM1215 [47] human colon cancer cell lines. The BaF/ERX cell line is an EGF-dependent cell line derived from BaF/wtEGFR [46] by continuous selection in EGF (F. Walker et al., in preparation). These cells display approximately 50,000 EGF receptors per cell but no other EGFR family member [46]. They respond mitogenically to EGF and therefore offer an assay system which is totally specific for the EGFR. They also respond mitogenically to IL3, allowing this signalling pathway to be used as a control for inhibitor specificity and toxicity.

The LIM1215 cell line [47] was originally derived from a patient with inherited non-polyposis colon cancer. These cells express approximately 40,000 EGF receptors per cell, but also low levels of ErbB2. They are therefore representative of the receptor heterogeneity likely to be encountered in the clinical situation.

The BaF/ERX cells were routinely cultured in RPMI 1640 supplemented with 10% fetal calf serum and 1% WEHI3 conditioned media (as a source of IL3). Prior to assay, the cells were washed three times and resuspended in RPMI 1640 supplemented with 10% FCS. Using an automated workstation (Biomek 2000, Beckman) cells were seeded into 96 well microtitre plates (Nunc) at 2×10^4 cells per 200 μl and incubated for 3 h at 37 °C, 5% CO_2. AG1478 samples were then added to the plates at a starting concentration of 5 μM and titrated two-fold. Mitogenic stimuli (5 ng/ml EGF or 1% IL3) were added to the AG1478-exposed and control cells. Cells were pulsed with 1 μCi/well ^{3}H-thymidine for 18 h at 37 °C, 5% CO_2 then harvested onto plates (Unifilter 96GF/C, Perkin-Elmer). The filter plates were dried and 20 μl of scintillation

cocktail (Microscint 20, Perkin-Elmer) was added per well and the plates counted in a 96 well plate counter (TopCount NXT, Perkin-Elmer). ^{3}H-thymidine incorporation was determined in counts per minute (cpm).

Assays using LIM 1215 cells were performed as above except that the cells were initially grown to confluence, trypsinised and resuspended in RPMI 1640 with ATG supplement (bovine serum albumin, iron saturated transferrin and L-glutamine). The cells were then seeded into 96 well microtitre plates at 5×10^4 cells per well using the automated workstation.

2.4. Cytosensor microphysiometry

Adherent LIM1215 [47] or non-adherent BaF/ERX cells [46] were embedded in 0.2% low gelling temperature agarose (5×10^5 cells) and seeded onto the polycarbonate membranes of each Cytosensor transwell capsule cup (Corning Transwell; 3 μm pore size, 12 mm diameter). Upon setting, a low buffering capacity running medium (DMEM with 5.5 mM glucose, 0.01% BSA containing the antibiotics penicillin and streptomycin) was added to the centre and outside of each capsule cup. A spacer was placed in the buffer directly over the cells and sandwiched by the transwell insert. The completed cell capsule assemblies were then transferred to the sensor chambers of the microphysiometer (Cytosensor, Molecular Devices, USA) which had been warmed to 37 °C and flushed with running buffer. Cells were equilibrated until a steady state extracellular acidification (ECAR) was obtained before exposure to reagents.

A 2 min pump cycle was established consisting of a 90 s pumping phase to equilibrate the system followed by a pump-off period of 30 s during which time the extra-cellular acidification rate (ECAR) was measured. The flow during the pump-on phase was 100 μl/min. The rate data were normalised to a percentage figure to account for slight channel to channel variations in cell number. The ECAR was determined from the slope of a linear-least squares fit to the plot of millivolts versus time during the pump-off cycle. The percentage change above or below basal rate is plotted against time and gives a quantitative measurement of the response of applied reagents. AG1478 was dissolved in DMSO and then diluted into tissue culture medium prior to perfusion for either the duration of the experiment or for a 30 min period prior to challenge with EGF. All EGF perfusions were a single pulse lasting three pump cycles (total 6 min).

2.5. RP-HPLC analysis

AG1478 levels in plasma were quantitated using a validated RP-HPLC method [48]. Briefly, plasma samples (90 μl) were extracted with acetonitrile-containing 50 mM internal standard (AG1557) and, following centrifugation, the supernatant was evaporated to dryness, reconstituted in 50% (v/v) acetonitrile:water and separated by HPLC (model 2690, Waters Australia) using a Symmetry C8 column (150 × 3 mm i.d., 5 μm, Waters Australia). A linear 38 min gradient of 10–90% acetonitrile in 0.1 M ammonium acetate buffer pH 6.0 over 38 min at a flow rate of 0.2 ml/min was used to elute the column. The column temperature was 25 °C and detection was at 330 nm. Inter- and intra-assay accuracy and precision were better than ±10% and the limit of quantitation was 0.2 μM.

For the chromatographic determination of levels of AG1478 in tissues, animals were humanely killed by cervical dislocation at 60 min following subcutaneous injection, and tissue removed and immediately frozen in liquid nitrogen and stored at −70 °C. Prior to extraction, tissue was thawed and weighed. Approximately 200–300 mg of sample was chopped and homogenised in 2 ml phosphate buffered saline before 2 ml of dichloromethane (Aldrich, MI, USA) was added and the sample vortexed and then centrifuged (5 min at 3000 × *g*). The organic phase was removed and the extraction repeated with a further 2 ml of dichloromethane, and the organic phases pooled and dried under helium and reconstituted in 50 μl DMSO for HPLC analysis. AG1478 was analysed using the RP-HPLC method described above with the following exceptions: an Aquapore RP 300 column (100 × 2.1 mm i.d., Perkin-Elmer, Australia) was installed in a Agilent Model 1100 HPLC (Agilent Technologies, Melbourne, Australia) and a linear 40 min gradient from 10% to 95% acetonitrile in 0.1 M ammonium acetate buffer pH 6.0 at a flow rate of 0.1 ml/min was used.

2.6. Tissue distribution studies

All animal studies were approved by the appropriate institutional Ethics Committees. To estimate tissue distribution, female BALB/c mice (20 g) were administered ^{3}H-AG1478 (5 μCi) in a carrier solution of 10 mM AG1478 tartrate in Captisol® (300 μl) by subcutaneous injection. At 25 min, 100 μl of technetium 99-labelled human serum albumin solution (^{99m}Tc-HSA) was injected via the tail vein. At 30 min, under Penthrane® anaesthesia, blood, tissue and organs were harvested, including liver, kidney, spleen, lung, heart, brain, muscle, stomach, small intestine, large intestine and skin. Tissues were trimmed of excess fat and connective tissue (intestine contents were emptied), rinsed briefly in 0.9% saline and blotted dry. Samples (100–300 mg) were homogenised in 300 μl of saline per 100 mg of sample. One 100 μl aliquot was counted immediately for ^{99m}Tc activity using a multi-detector gamma counter (Wizard 1470, Wallac, Finland). A second 100 μl aliquot (or 50 μl of blood) was solubilised with 0.5 ml of tissue solubiliser (NCS, Amersham, IL, USA) by heating at 60 °C for 1 h. The soluble homogenate was cooled to room temperature and following addition of 6 ml of scintillation cocktail (Optiphase HiSafe3, LKB, Leics, UK) was counted for beta activity (Tricarb 2100TR, Packard, CT, USA) immediately and then recounted after 60 h (greater than 10 times the half-life of ^{99m}Tc) to ensure that any weak beta emission from the ^{99m}Tc isotope did not contribute to the assessment of activity of the ^{3}H label of AG1478. Injected solutions were also counted to calculate the total dose.

The volume of blood in each tissue homogenate was calculated by relating the gamma activity (^{99m}Tc-HSA) for a known volume of blood to the gamma activity for the homogenate. The ^{99m}Tc-HSA is retained within the vasculature during the deliberately short (5 min) distribution time. The ^{3}H-AG1478 content of each tissue was calculated by subtracting the beta activity for the blood component from that for the complete homogenate.

Table 1 – Prototype formulations used

Formulation	Dose administered
MICE: s.c. and p.o. bolus	
AG1478 tartrate in Captisol® (μmol/kg)	136 and 272
AG1478 citrate in Captisol® (μmol/kg)	780
RATS: intravenous	
AG1478 mesylate in Captisol®	
Bolus (μmol/kg)	9.5, 19.0, 47.5 and 95.0
Steady state infusion (1 ml/h) (μmol/kg/h)	24, 111 and 161

2.7. Pharmacokinetic studies

2.7.1. Mice: subcutaneous and oral bolus studies

AG1478 was delivered as a single subcutaneous (s.c) or oral (p.o.) dose in less than 30 s at a volume of 15 ml/kg to female BALB/c mice. Doses were 136 and 272 μmol/kg as the tartrate salt and 780 μmol/kg as the citrate salt, in Captisol® formulation (Table 1). Blood was sampled at selected times from 5 to 480 min by axillary dissection under terminal Penthrane® anaesthesia. Plasma was obtained by centrifugation and aliquots were stored at −70 °C prior to RP-HPLC analysis.

2.7.2. Rats: intravenous pharmacokinetics and steady state infusion studies

Under isofluorane anaesthesia, the carotid artery (for blood samples) and jugular vein (for drug dosing) of male Sprague-Dawley rats (280–320 g) were cannulated using polyethylene tubing (0.96 mm o.d., 0.58 mm i.d.) [49]. The cannulae were left subcutaneously until being exteriorised just prior to dosing on the following day. Rats returned to normal grooming, drinking and sleeping behaviour within 1 h of surgery. On the day of dosing rats were housed in cages fitted with swivel attachments to enable free movement while protecting the cannulae.

AG1478 was administered over 5 min (bolus dose, 2 ml), or infused over 6 h at 1 ml/h using a syringe driver (Model MS 16A, Graseby Medical) using the formulations described in Table 1. Control animals received Captisol® vehicle only. Heparinised blood samples (0.2 ml) were collected predose and at multiple times. A 150 μl aliquot of plasma was stored at −20 °C until RP-HPLC analysis, which was conducted within 2 weeks.

2.8. Pharmacokinetic calculations

The area under concentration time curves ($AUC_{0\rightarrow\infty}$) was calculated using the linear trapezoidal rule up to the last measurable concentration. The extrapolated terminal elimination area was determined by dividing the last measured concentration by the terminal elimination rate constant. The following equations were employed to calculate the apparent volume of distribution (V_d), half-life ($t_{1/2}$) and the total clearance (Cl), respectively:

$$V_d = \text{dose}(\mu g)/(\text{elim. rate constant}(\text{min}^{-1}) \times AUC_{0\rightarrow\infty}(\mu g\,\text{min/ml}))/\text{weight(kg)},$$

$$t_{1/2} = \ln 2/\text{elim. rate constant},$$

$$Cl = \{\text{dose}(\mu g)/AUC_{0\rightarrow\infty}(\mu g\,\text{min/ml})\}/\text{weight(kg)}$$

2.9. Inhibition of EGFR activity in mouse tumour xenografts

U87MG.Δ2-7 glioblastoma cells (23, 24) in 100 μl of PBS (3×10^6 cells) were injected s.c. into both flanks of 4–6-week-old, female nude mice (Animal Research Centre, Perth, Australia). All studies were conducted using established tumour models. Treatment commenced once tumours had reached a mean volume of approximately 70 mm^3. Mice bearing xenografts were injected intraperitoneally with AG1478 at 50 or 125 μmol/kg on days 1, 3, 5, 7, 9 and 11. The mice were monitored to day 24. They were then given one final injection of AG1478 30 min prior to sacrifice. The tumours were harvested and snap-frozen in dry ice for the determination of EGFR activation and signalling. Frozen tumour samples were thawed, chopped manually and resuspended in RIPA buffer-containing protease and phosphatase inhibitors. Tissues were disrupted by sonication, and lysates cleared of insoluble material by high-speed centrifugation. The protein content of the solubilised samples was determined by the BCA method (Pierce Biotechnology, Rockford, IL). Equivalent amounts of each sample were separated by SDS-PAGE and transferred to Immobilon membranes (Millipore, Billerica, MA). EGFR activation was assessed by probing the membranes with anti-phosphotyrosine antibody 4G10 (Upstate, Waltham, MA) and anti-EGFR antibody 806 [40,50]. For the determination of EGFR downstream signalling to the MAPK pathway, membranes were probed with anti-phospho MAPK antibody (Cell Signaling Technology Beverly, MA) and re-probed with a pan-ERK antibody (Santa Cruz Biotechnology, Santa Cruz, CA). Reactive bands were visualized using HRP-coupled secondary antibodies (BioRad, Hercules, CA) followed by enhanced chemiluminescence (ECL: Amersham Bioscience, Piscataway, NJ). Densitometric analysis of the reactive bands was performed using a Molecular Dynamics computing densitometer and ImageQuant software (Molecular Dynamics, Sunnyvale, CA). Specific EGFR phosphorylation is defined as the ratio of phospho-EGFR to total EGFR protein; similarly, MAPK activation is defined as the ratio of phosphorylated MAPK to total MAPK protein. AG1478 levels in blood and tumours were determined by RP-HPLC as described above.

3. Results

3.1. Formulation

The maximum concentrations obtained for AG1478 free base and salts in both water and Captisol® are reported in Table 2. The formation of the chloride, citrate, tartrate or mesylate salts of AG1478 gave significant increases in the aqueous solubility (225, 440 μM, 1 and 37 mM, respectively). The maximum concentration of AG1478 free base in DMSO was 200 mM whereas in de-ionised water at ambient temperature (25 °C) the maximum solubility is reduced by a factor of 10^4. Captisol® increased the aqueous solubility approximately 200-fold (to 400 μM) over water alone (Table 2). Similarly, the use of Captisol® resulted in further increases in solubility for the salt forms of AG1478 (to 35, 50, 50 and 90 mM, respectively: Table 2). The AG1478 mesylate salt at 49 mM in Captisol®

Table 2 – Concentrations achieved using A1478 salts compared to free base

Solvent	Concentrations of AG1478 (mM) achieved				
	Base	Chloride	Citrate	Tartrate	Mesylate
Water	0.00195	0.225	0.440	1	37
Captisol®	0.4	35	50	50	90
DMSO	200				

(98 mM) was chosen as the final formulation. Typically, cyclodextrins have been found to form 1:1 or 1:2 inclusion complexes [45]. Whilst preliminary experiments showed that a 1:1 formulation gave effective solubilisation, long term solubility was improved if a 1:2 mixture was used.

3.2. Mitogenic analysis

The potency of the AG1478 preparations was calculated from the inhibition of tritiated thymidine uptake by either the Baf/ERX cell line (generated by transfection of the murine pre-B BaF/3 cell line, which has no endogenous members of the EGFR family, with EGFR [46]) or LIM1215 colon carcinoma cells [47] following challenge with a dose of EGF (0.8 nM) which caused maximal stimulation. The observed IC_{50} using the BaF/ERX cells was approximately 0.07 μM (Fig. 2A). The potency for the LIM 1215 human colon cancer cell line [47] (IC_{50} = 0.2 μM, Fig. 2B) was slightly reduced.

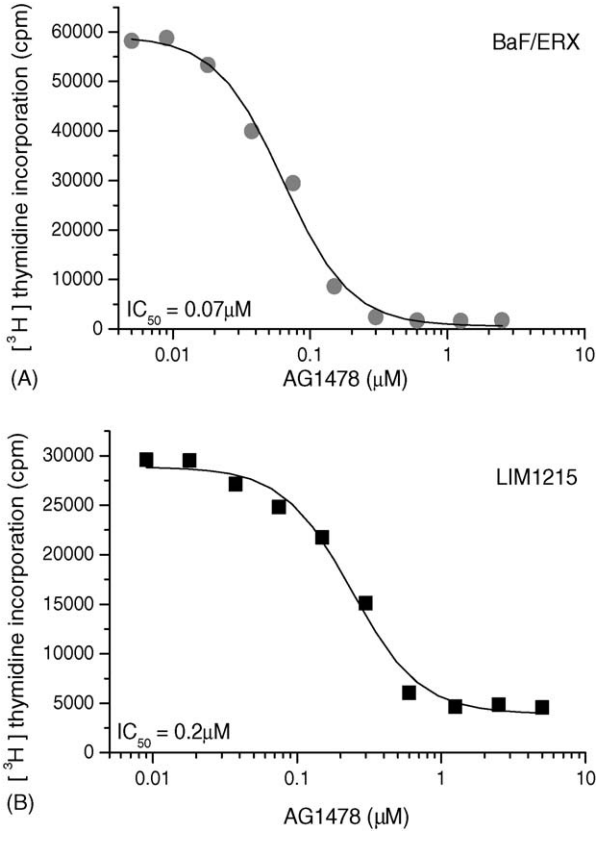

Fig. 2 – Inhibition of EGF-dependent ^{3}H-thymidine incorporation by AG1478. BaF/ERX (panel A) or LIM1215 cells (panel B) were incubated with AG1478 at the doses indicated prior to stimulation with EGF (0.8 nM) in the presence of ^{3}H-thymidine as described in Section 2. The IC_{50} was calculated by fitting the incorporated counts recovered (solid symbols) to a sigmoid function (—) using Origin (OriginLab Corporation, Northampton, MA, USA).

3.3. Microphysiometer analyses

The microphysiometer (Cytosensor, Molecular Devices, USA) uses a silico-based light addressable potentiometric sensor to make rapid (<30 s), sensitive (>0.01 pH units) and precise measurements of extracellular pH following cell stimulation [51]. Cells are maintained in a transwell assembly above the detector. Measurements are made of the rate at which the cells secrete acidic by-products (extracellular acidification rate, ECAR) due to metabolic and regulatory events within the cell. This instrument has been used previously to monitor EGF/EGFR family interactions [52–55].

A rapid increase in extracellular acidification was observed following stimulation of BaF/ERX cells with a pulse of EGF (6 min duration), which decayed back to baseline over the next 2–3 h (Fig. 3A). Re-stimulation at this time (data not shown) gave a similar response. If the cells were treated with AG1478, the response was inhibited in a dose-dependent manner (Fig. 3A). The IC_{50} was approximately 0.3 μM in this assay. The LIM1215 colonic carcinoma cell lines showed a similar response to EGF (Fig. 3B, EGF control) and gave similar inhibition with the AG1478 (data not shown).

The microphysiometer was also used to determine the duration of inhibition following exposure to AG1478 using the LIM1215 cells (Fig. 3B). The cells were pre-treated with AG1478 (5 μM) for 30 min, a dose which caused maximal inhibition (Fig. 3A). The inhibitor was then removed and the cells challenged at various time intervals with EGF (100 ng/ml). Cells exposed to EGF at 0, 12 and 18 min post-removal of the inhibitor did not respond instantaneously to EGF challenge. However, a significant delayed response was seen in all cells around 24 min. Cells challenged 24 min after removal of the inhibitor showed immediate response.

3.4. Tissue distribution

Tissue distribution of AG1478 was determined following subcutaneous injection of ^{3}H-AG1478. Results were corrected for blood pool contamination using ^{99m}Tc-HSA injected just 5 min prior to sacrifice. ^{99m}Tc-HSA has a short half-life and will be retained within the vasculature because of the short time between the injection of this tracer and sacrifice of the animal. Tissue levels of ^{3}H-AG1478, assessed 30 min after injection, were highest in the liver, kidney and muscle at 6.3%, 3.9% and 4.1% of the dose, respectively (Fig. 4). Approximately 4.1% of the dose was retained in the blood at this time. The

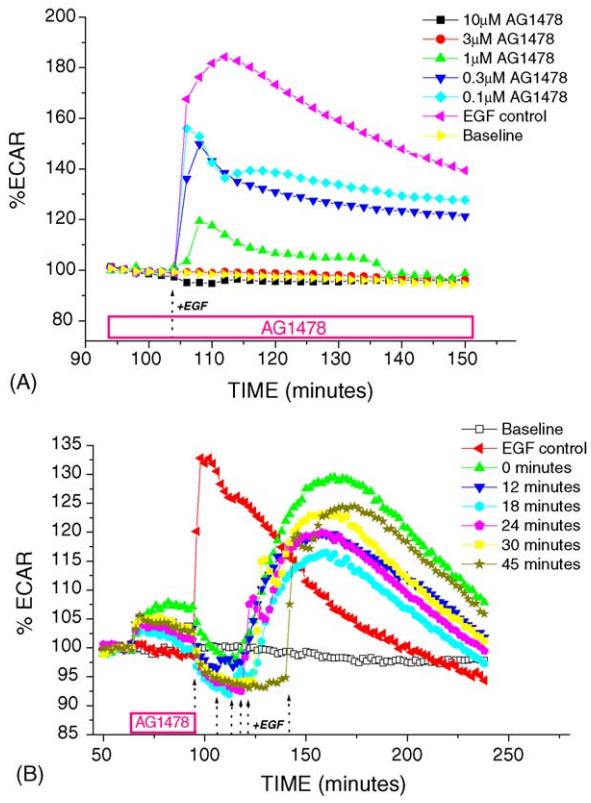

Fig. 3 – Analysis of AG1478 inhibition of EGF-induced cell stimulation using a Cytosensor Microphysiometer. (A) Dose-dependent inhibition by AG1478. BaF/ERX cells were inhibited with AG1478 as indicated and the extracellular acidification rate (ECAR) measured, as described in Section 2, following stimulation with EGF (16 nM). (B) Duration of AG1478 inhibition. LIM1215 cells were pre-incubated with AG1478 (5 μM) for 30 min. The inhibitor was then removed and the cells challenged with EGF (16 nM) at the times indicated.

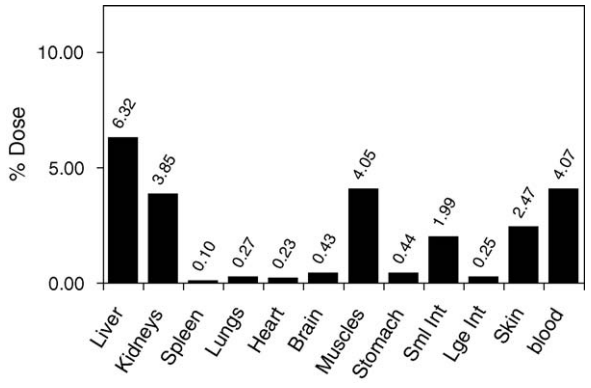

Fig. 4 – Tissue distribution of ^{3}H-AG1478 in a mouse at 30 min after subcutaneous bolus dose. Tissue levels of ^{3}H-AG1478, expressed as percent of the dose administered, were corrected for blood content that was measured using ^{99}Tc-labelled human serum albumin.

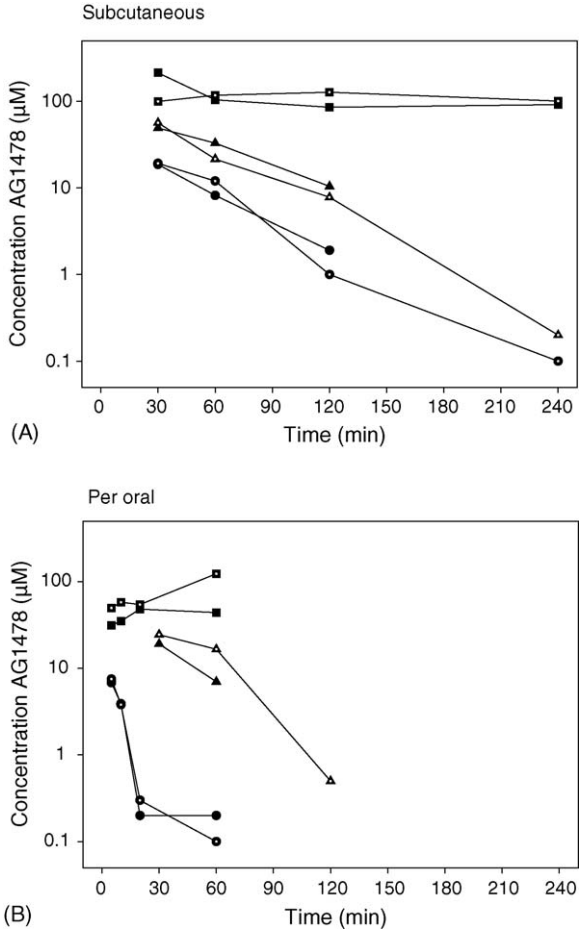

Fig. 5 – Semilogarithmic plot of plasma AG1478 elimination in mice following subcutaneous (A) and oral (B) doses of 136 μmol/kg (circle) and 280 μmol/kg (triangle) AG1478-citrate or 780 μmol/kg (square) AG1478-tartrate using Captisol®/aqueous formulations. Each time point corresponds to one individual mouse.

other tissues, including brain, showed levels between 0.1% and 0.5% of the dose. The total recovery of the administered dose was 34%. Bile, faeces, urine or intestinal contents were not collected for analysis. Similar tissue distribution was observed when tissue AG1478 levels were measured by RP-HPLC following a comparable dose of non-radiolabelled AG1478 (data not shown), allowance being made for blood pool volumes.

3.5. *Pharmacokinetics*

3.5.1. *Mice: subcutaneous and oral studies*

A subcutaneous (s.c.) dose of 780 μmol/kg AG1478 resulted in signs of mild toxicity (hunched posture and shallow breathing). Examination of the corresponding plasma concentrations indicated sustained, elevated AG1478 levels of around 100 μM over the 4 h period measured (Fig. 5). This high plasma level suggested that much lower doses would be sufficient to give AG1478 plasma levels that were capable of blocking the EGFR signalling pathways. Doses of 136–272 μmol/kg were therefore investigated. These doses resulted in initial serum plasma

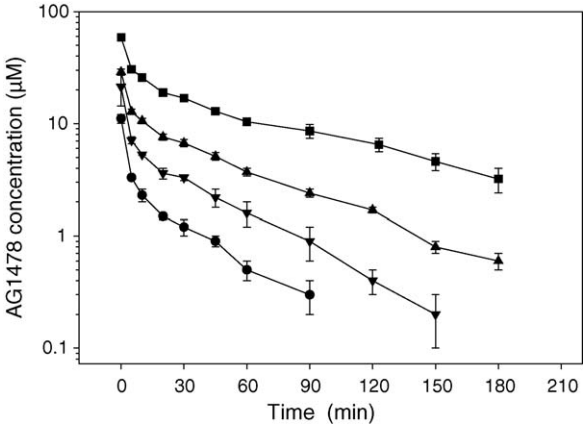

Fig. 6 – Semilogarithmic plot of mean (±S.E.M., $n \geq 3$) plasma AG1478 elimination in rats after intravenous dose of 9.5 (circle), 19.0 (triangle down), 47.5 (triangle up) or 95.0 (square) μmol/kg AG1478 administered over 5 min.

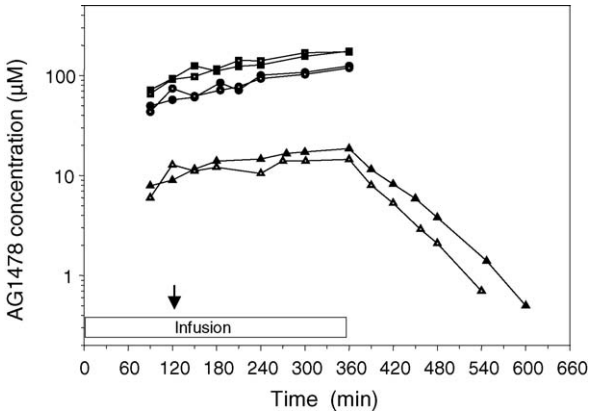

Fig. 7 – Semilogarithmic plot of plasma AG1478 levels during and post 6 h intravenous infusions of AG1478-mesylate in Captisol® 24 (triangle up) 111 (circles) and 161 (squares) μmol/kg/h. The data presented is from two rats per dose level. The time of attainment of theoretical steady state (120 min) is indicated by an arrow. Blood samples were not taken post-infusion in the 111 or 161 μmol/kg/h experiments.

levels of >20 μM (Fig. 5). The two-fold dose escalation resulted in a 2.4-fold increase in the total AUC (from 32.6 to 80.8 μmol h/ml). The elimination from plasma was monoexponential with a half-life of 30 min (Fig. 5A).

Oral administration of the 780 μmol/kg AG1478 dose also resulted in mild toxicity with sustained plasma concentrations of AG1478 >40 μM (Fig. 5B). Following oral administration relatively high plasma concentrations were reached by the first sample time (5 min) suggesting rapid absorption. Oral administration resulted in similar AG1478 elimination from plasma with generally lower peak plasma concentrations for each dose compared to subcutaneous administration (Fig. 5).

3.5.2. *Rats: intravenous studies*

(i) *Bolus i.v.* The use of rats as an experimental model facilitated studies using an intravenous route of administration, which is more akin to the proposed clinical situation, and permitted pharmacokinetic sampling without requiring the sacrifice of an animal for each time point. There were no adverse effects evident following bolus i.v. administration of AG1478 to rats at any of the four doses examined (between 9.5 and 95.0 μmol/kg). High plasma levels (10–60 μM) were evident at the first measured time point (2.5 min) which then declined in a biphasic manner with a terminal elimination half-life of 30–48 min (Fig. 6, Table 3). There were no significant differences between $t_{1/2}$, V_d or Cl. A linear relationship between dose and $AUC_{0\rightarrow\infty}$ ($r^2 = 0.979$) indicated non-saturable conditions thereby allowing prediction of an infusion rate and dose for continuous infusions.

(ii) *Steady state infusion.* The data obtained with the bolus injections suggested that 120 min (approximately four elimination half-lives) should be allowed for the attainment of steady state. A total infusion time of 6 h was chosen using doses of 24, 111 and 161 μmol/kg/h. Steady state appeared to be reached by 120 min as predicted, although there was a further gradual increase in plasma concentrations with time in each rat at all doses used (Fig. 7). The sustained AG1478 plasma concentrations ranged from approximately 10–100 μM, depending on the dosage administered. Following infusion at the lowest dose, plasma drug levels declined with a half-lives of approximately 43 min (rat 1 = 42.6 min; rat 2 = 44.5 min). At both of the higher infusion concentrations (111 and 161 μmol/kg/h), the experiments were terminated at 360 min due to adverse effects (lethargy accompanied by the inability of the rat to support its own weight) relative to a "control" rat that received an infusion of the Captisol® vehicle only.

Table 3 – Pharmacokinetic parameters after intravenous administration over 5 min in rats dosed with AG1478 in Captisol®

Target dose (μmol/kg)	Actual dose (μmol/kg)	n	$AUC_{0\rightarrow\infty}$ (nmol h/ml)	$t_{1/2}$ (min)	Vol. dist. (l/kg)	Clearance (ml/min/kg)
9.5	9.5 ± 0.3	3	3.6 ± 0.3	30.9 ± 8.6	2.6 ± 0.9	58.3 ± 5.9
19.0	18.7 ± 0.6	3	9.2 ± 2.1	28.9 ± 2.2	2.3 ± 0.7	55.1 ± 17.0
47.5	48.4 ± 1.2	4	14.3 ± 1.1	43.1 ± 7.7	3.6 ± 0.8	56.9 ± 5.5
95.0	93.1 ± 3.8	3	38.5 ± 4.9	48.2 ± 28.5	2.8 ± 1.4	40.8 ± 3.6

Mean ± S.D. and $n \geq 3$.

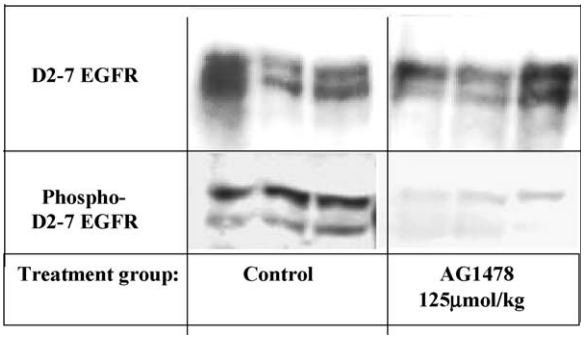

Fig. 8 – U87MG.Δ2-7 xenografts from three untreated mice (controls) or three mice treated with AG1478 at 125 μmol/kg (as described in Section 2) were harvested 30 min after the last injection of AG1478. Tumours were processed as described in Section 2, and equal amounts of protein were analysed by SDS/PAGE. Total Δ2-7 EGFR protein (upper panel) and tyrosine-phosphorylated protein (lower panel) were detected by immunoblotting with specific antibodies as described in Section 2.

3.6. *Inhibition of EGFR activation and downstream signalling in tumours from AG1478-treated mice*

Mice bearing xenografts of the human glioblastoma cell line U87MG.Δ2-7, which expresses a constitutively active variant of the EGF receptor [23], were injected with AG1478 in Captisol®, at either 50 μmol/kg ($n = 4$) or 125 μmol/kg ($n = 4$) (six doses over 11 days as described in Section 2). Tumour growth was monitored to day 24. Mice were sacrificed 30 min after the last injection. Tumour samples, as well as blood samples, were collected for parallel determination of inhibition of EGFR signalling and of AG1478 levels in the samples (Fig. 8, Table 4). EGFR activation status in tumour samples was monitored by measuring both the specific tyrosine phosphorylation of the EGFR (Fig. 8), and the Ser/Thr phosphorylation of MAPK proteins. MAPK phosphorylation is a more sensitive readout of EGFR activation than EGF phosphorylation itself and parallels more directly the cellular effects of EGFR activation [56]. Inhibition of EGFR signalling was dose-dependent (Table 4): administration of 125 μmol/kg AG1478 resulted in tumour levels of 0.042 μmol AG1478 per g of tissue, which was sufficient to virtually totally abolish EGFR activation (Fig. 8 and Table 4).

4. Discussion

The EGFR family is abnormally activated in many epithelial cancers. The development of specific potent inhibitors of this signalling pathway as a target for anticancer therapy is therefore an active and ongoing area of research. The quinazoline AG1478 [30,31,48] is a highly potent and specific small molecule inhibitor of the EGFR (ErbB1), inhibiting EGF-induced mitogenesis of the BaF/ERX or LIM1215 cell lines with an IC_{50} of 0.07 or 0.2 μM, respectively (Fig. 2).

The duration of effective inhibition by AG1478 of EGF-induced response was assessed in the Cytosensor microphysiometer [51–55]. A delayed cell signalling of up to 18 min following withdrawal of the inhibitor if challenged with EGF was observed (Fig. 3). HPLC analysis (data not shown) had indicated that AG1478 was stable in culture over this time period. The delayed signalling is therefore most probably due to diffusion of the inhibitor from the ATP binding site while EGF is still bound to, and activating, the receptor. Cells showed an immediate response if challenged with EGF 24 min after withdrawal of the inhibitor. This suggested that in vivo the AG1478 levels would need to be maintained at constant effective levels over a period of time.

The rational design of dose regimens for administration of AG1478 in clinical trials must be underpinned by an understanding of its pharmacokinetic behaviour in animal models. For such studies, an appropriate safe pharmaceutical formulation must be available in order to study the compound at relevant concentrations. However, to date the use of AG1478 has been limited by its limited aqueous solubility. In previous in vivo studies [23,39], AG1478 was delivered using 20–50 μl of dimethylsulfoxide (DMSO) as the vehicle for each injection. Although this is below the dose of DMSO known to cause toxicity with a repeat injection regime in mice [57], there is clearly a need to find an alternative formulation if AG1478 is to be useful as a clinical agent: currently DMSO is only approved by the FDA for palliative treatment of interstitial cystitis and for limited veterinary use, and has been reported to have a number of unpleasant side effects including excretion as dimethyl sulfide which has an unpleasant odour.

Drugs of low water solubility intended for parenteral administration are typically solubilised by pH-control, use of pharmaceutical salts, co-solvency or emulsification. Solubilisation attempts using non-aqueous co-solvents (propylene glycol, ethanol and water) resulted in unstable formulations (data not shown). Complexation between the drug and the

Table 4 – Inhibition of EGFR signalling and AG1478 levels in xenografts from mice injected with different doses of AG1478

Assay	Vehicle control	AG1478 (50 μmol/kg)	AG1478 (125 μmol/kg)
Specific MAPK activation	0.041 ± 0.021	0.022 ± 0.018	0.011 ± 0.006
Specific EGFR phosphorylation	1.73 ± 0.62	1.09 ± 0.08	0.71 ± 0.16
AG1478 in tumours (μmol/g)	0	0.013 ± 0.005	0.0421 ± 0.016
AG1478 in blood (μM)	0	22.5 ± 5	60.1 ± 12

Mice carrying U87MG.Δ2-7 xenografts were injected IP with AG1478 at the doses indicated. Tumours were harvested 30 min after injection and analysed for EGFR activation and MAPK activation. Phosphorylated and total protein levels were determined by SDS/PAGE and immunoblotting with specific antibodies as described in Section 2. Reactive bands were quantitated by scanning densitometry. Tumour and blood samples collected at this time were also analysed for levels of AG1478 as described in Section 2. Data represent means and standard deviations of four independent samples.

Captisol® excipient is a feasible alternative where the increase in solubility of the drug is a result of an inclusion complex formed between the guest molecule (drug) and the host (Captisol®). Although the entire cyclodextrin molecule is water soluble, the interior of the molecule is relatively apolar, and creates a hydrophobic microenvironment with the ability to encapsulate hydrophobic, insoluble molecules [45]. Captisol® has been approved for clinical use by the US Food and Drug Administration as the excipient for at least two injectable drugs: an antipsychotic agent (Geodon, Pfizer) and an antifungal agent (Vfend, Pfizer).

A combination of the mesylate salt of AG1478 with formulation in Captisol® allowed concentrations of up to 90 mM to be achieved (Table 1). Vehicle control experiments in mice, where Captisol® was administered alone, confirmed no evidence of toxicity at the doses used. This formulation was well tolerated and not only avoided the potential toxicity problems of solvent-based excipients such as dimethylsulfoxide or ethanol, but also overcame the problem of drug precipitation observed with non-Captisol® aqueous-based excipients.

Preliminary in vivo pharmacokinetic characterisation of AG1478 was performed using mice and rats following bolus administration. These studies revealed little difference between mice and rats in the elimination of AG1478 from the plasma. In rats the peak plasma concentration was attained rapidly, in the sample taken immediately following the end of the 5 min 'bolus' infusion, and in mice, at doses below 780 μmol/kg, the peak plasma concentration was achieved at the first sample point. For bolus doses below 780 μmol/kg, the plasma profile of AG1478 in both rat and mouse showed typical log-linear elimination. An exception was noted following oral administration to mice where plasma levels although variable, appeared to decrease rapidly. This could however have resulted from differences in absorption or first pass effects between the two routes. The rapid elimination from plasma was consistent with the low tissue and plasma levels observed when tissue distribution of bolus radiolabelled AG1478 was assessed. The elimination of AG1478 from the plasma of rodents would appear to be more rapid than for gefitinib which, albeit at lower doses (C_{max} of 5.6–6.9 μM), displays an apparent plasma elimination half-life of approximately 3.2 h in mice following a prolonged oral dosing regimen of 50 mg/kg (112 μmol/kg) daily for 4 days [58]. The more rapid elimination of AG1478 suggested that the use of continuous i.v. infusion over an oral dosing regimen was required to rapidly achieve and maintain high plasma levels. The observed constant plasma level of AG1478 following the highest dose of 780 μmol/kg using either oral or subcutaneous routes may indicate a failure of elimination mechanisms when considered in conjunction with the occasionally observed behavioural signs of toxicity at this dose. Intravenous bolus administration in rats achieved high (>10 μM) initial plasma levels of AG1478 that were similar to those seen in the mice but were achieved using lower doses (9.5–95.0 μmol/kg compared to 136–272 μmol/kg).

Demonstration of a drug effect on the proposed molecular target (in this case the EGFR) is highly desirable but is often impractical due to inaccessibility of the tumour tissue. In the mouse, tritiated AG1478 was widely distributed at low levels throughout the sampled tissues 30 min after a bolus subcutaneous dose. The large proportion of the administered dose of ^{3}H-AG1478 that was not recovered in tissues or blood was considered likely to have resulted from hepatic and or renal excretion (not assessed in this study).

Fredriksson et al. [59] have studied the biodistribution of ^{11}C-labelled 4-(3-bromoanilino)-6,7-dimethoxyquinazoline (PD153035, the bromoanilino analogue of AG1478) in rats using positron emission tomography. These data indicated that the radiotracer was rapidly cleared from plasma with subsequent uptake in the brain, heart, liver, gastrointestinal tract and bladder. McKillop et al. reported gefitinib tissue distribution to be similarly extensive in both mice and rats following oral administration, with the levels of gefitinib in tissues generally higher than in blood when measured between 2 and 8 h after prolonged oral dosing (50 mg/kg (112 μmol/kg) per day for 4 days) [58]. The tissue distribution and levels of AG1478 achieved within 30 min of a single bolus dose in our studies was generally consistent with the above data: differences in the dose regimens and drug metabolism pathways may account for the slight differences such as the distribution to brain and the lower total recovery seen with AG1478. The metabolic fate of AG1478 in rats and mice is currently under investigation (E. Nice et al., unpublished data).

The pharmacokinetic data obtained from the bolus dose studies in rats enabled the rational design of infusion experiments, enabled the rational design of infusion experiments, in concordance with the microphysiometry data to achieve steady state plasma levels of around 10 μM. This level was chosen since it was significantly above the IC_{50} levels determined in our mitogenic and cytosensor assays, and, most importantly because experiments on skin and brain samples obtained from mice post-administration of AG1478, where the serum concentration had been analysed by RP-HPLC, had shown that these levels were capable of totally inhibiting EGFR and MAPK phosphorylation (data not shown). The levels achieved during infusion were consistent at each of the doses used although a slight trend for increasing concentration over time was observed. Experiments were ceased at the end of infusion with the two higher doses due to occasionally observed behavioural signs of toxicity. At the lowest dose, a level of approximately 10 μM could be maintained in the absence of any observed behavioural effects. Intravenous delivery can avoid the variability associated with altered oral bioavailability. Indeed clinically the mean oral bioavailability of erlotinib following a 150 mg (349 μmol) oral dose has been reported to increase from 59% to almost 100% by taking it with food [60]. Furthermore the plasma concentrations of gefitinib can be reduced by co-medications such as ranitidine and cimetidine that can cause significant sustained elevation of gastric pH [60].

To further confirm the ability of the circulating serum levels of AG1478 to reach the tumour target, and shut down the relevant signalling pathways, we have tested the efficacy of AG1478 administered ''in vivo'' against U87MG.Δ2-7 glioblastoma xenografts. The Δ2-7 EGFR variant, which is expressed in a high proportion of human glioblastomas [23,35,38], is constitutively activated, albeit at a low level, resulting in increased proliferation and survival of the tumour cells and therefore represents a useful model of EGFR-dependent

tumour development. Bolus administration of AG1478 at relatively low doses resulted in significant uptake by the tumours, which was accompanied by profound inhibition of EGFR-mediated activation and signalling (Fig. 8 and Table 4). The plasma levels of AG1478 in mice bearing tumour xenografts taken at 30 min post-dose were consistent with the plasma elimination profiles exhibited in the initial experiments in tumour free mice. The levels of AG1478 in tumour tissue at 30 min post 50 or 125 μmol/kg dose were 0.013 ± 0.005 and 0.0421 ± 0.016 μmol/g, respectively (Table 4). This was consistent with the reported tumour levels of gefitinib (0.025 ± 0.002 μmol/g) achieved in mice receiving 112 μmol/kg daily for 4 days [58]. Interestingly in that study, for both the plasma and tumour tissue levels of gefitinib taken 2–8 h after dosing of mice and measured by either radioactivity or HPLC-MS/MS there was no difference between single or multiple (daily for 4 days) oral dosing regimes.

When trialled as monotherapy, and assessed by survival advantage compared to placebo in non-small cell lung cancer, gefitinib and erlotinib had different outcomes [61,62]: gefitinib showed no survival advantage [61] whilst erlotinib showed improved survival of 2 months compared with patients receiving a placebo [62]. AG1478, whilst sharing the same structural quinazoline backbone as gefitinib and erlotinib (see Fig. 1), lacks the hydrophilic side chains which may confer significantly different properties. The availability of alternative inhibitors in novel formulations provides the opportunity to evaluate further the therapeutic potential of this important class of compounds.

5. Conclusions

These results confirmed the therapeutic potential of AG1478 and the feasibility of administering efficacious doses of the inhibitor by continuous infusion of aqueous formulations using Capitisol as an excipient. We have evaluated the pharmacokinetics in rodents, successfully achieving sustained plasma concentrations of >10 μM over 6 h. This represents a novel approach to the delivery of a specific reversible inhibitor of EGFR tyrosine kinase at levels which should be clinically relevant.

Acknowledgements

The authors would like to thank S. Rainone and N. Wark (Peter MacCallum Cancer Centre) for technical assistance and Peter Eu (Peter MacCallum Cancer Institute) for the preparation of the ^{99m}Tc-HSA. These studies were supported, in part, by National Health & Medical Research Council of Australia (NHMRC) Project Grants 191500, 164809 and 164814 and Program Grant 164802.

REFERENCES

[1] Burgess AW, Cho HS, Eigenbrot C, Ferguson KM, Garrett TP, Leahy DJ, et al. An open-and-shut case? Recent insights into the activation of EGF/ErbB receptors. Mol Cell 2003;12:541–52.
[2] De Bono JS, Rowinsky EK. Therapeutics targeting signal transduction for patients with colorectal carcinoma. Br Med Bull 2002;64:227–54.
[3] Yarden Y, Sliwkowski MX. Untangling the ErbB signalling network. Nat Rev Mol Cell Biol 2001;2(2):127–37.
[4] Kari C, Chan TO, Rocha de Quadros M, Rodeck U. Targeting the epidermal growth factor receptor in cancer: apoptosis takes center stage. Cancer Res 2003;63:1–5.
[5] Mendelsohn J, Baselga J. The EGF receptor family as targets for cancer therapy. Oncogene 2000;19(56):6550–65.
[6] Baselga J, Arteaga CL. Critical update and emerging trends in epidermal growth factor receptor targeting in cancer. J Clin Oncol 2005;23:2445–59.
[7] Tiseo M, Loprevite M, Ardizzoni A. Epidermal growth factor receptor inhibitors: a new prospective in the treatment of lung cancer. Curr Med Chem Anti-Canc Agents 2004;4:139–48.
[8] Li S, Schmitz KR, Jeffrey PD, Wiltzius JJ, Kussie P, Ferguson KM. Structural basis for inhibition of the epidermal growth factor receptor by cetuximab. Cancer Cell 2005;7:301–11.
[9] Wels W, Biburger M, Muller T, Dalken B, Giesubel U, Tonn T, et al. Recombinant immunotoxins and retargeted killer cells: employing engineered antibody fragments for tumour-specific targeting of cytotoxic effectors. Cancer Immunol Immunother 2004;53:217–26.
[10] Wells A. The epidermal growth factor receptor? A new target in cancer therapy. Signal 2000;1:4–10.
[11] Shaw JP, Akiyoshi DE, Arrigo DA, Rhoad AE, Sullivan B, Thomas J, et al. Cytotoxic properties of DAB486EGF and DAB389EGF, epidermal growth factor (EGF) receptor-targeted fusion toxins. J Biol Chem 1991;266:21118–24.
[12] Baselga J. Why the epidermal growth factor receptor? The rationale for cancer therapy. Oncologist 2002;7(Suppl. 4):2–8.
[13] Gosh S, Liu XP, Zheng Y, Uckun FM. Rational design of potent and selective EGFR tryrosine kinase inhibitors as anticancer agents. Curr Cancer Drug Targets 2001;1(2):129–40.
[14] Bridges AJ. The rationale and strategy used to develop a series of highly potent, irreversible inhibitors of the epidermal growth factor receptor family of tyrosine kinases. Curr Med Chem 1999;6:825–43.
[15] Powell TJ, Ben-Bassat H, Klein BY, Chen H, Shenoy N, McCollough J, et al. Growth inhibition of psoriatic keratinocytes by quinazoline tyrosine kinase inhibitors. Brit J Dermatol 1999;141:802–10.
[16] Shawver LK, Slamon D, Ullrich A. Smart drugs: tyrosine kinase inhibitors in cancer therapy. Cancer Cell 2002;1:117–23.
[17] Morin MJ. From oncogene to drug: development of small molecule tyrosine kinase inhibitors as anti-tumour and anti-angiogenic agents. Oncogene 2002;19:6574–83.
[18] Fukuoka M, Yano S, Giaccone G, Tamura T, Nakagawa K, Douillard JY, et al. Multi-institutional randomized phase II trial of Gefitinib for previously treated patients with advanced non-small-cell lung cancer. J Clin Oncol 2003;21:2237–46.
[19] Baselga J. Combined anti-EGF receptor and anti-HER2 receptor therapy in breast cancer: a promising strategy ready for clinical testing. Ann Oncol 2002;13:8–9.
[20] Shepherd FA, Pereira J, Ciuleanu TE, Tan EH, Hirsh V, Thongprasert S, et al. A randomized placebo-controlled trial of erlotinib in patients with advanced non-small cell lung cancer (NSCLC) following failure of 1st line or 2nd line chemotherapy. A National Cancer Institute of Canada Clinical Trials Group (NCIC CTG) trial. J Clin Oncol ASCO Ann Meet Proc (Post-Meet Ed) 2004;22(14S):7022.

[21] Denny W. Irreversible inhibitors of the erbB family of protein tyrosine kinases. Pharmacol The 2002;93:253–61.
[22] Raymond E, Faivre S, Armand JP. Epidermal growth factor receptor tyrosine kinase as a target for anticancer therapy. Drugs 2000;60(Suppl. 1):15–23.
[23] Nagane M, Narita Y, Mishima K, Levitzki A, Burgess AW, Cavenee WK, et al. Human glioblastoma xenografts overexpressing a tumour-specific mutant epidermal growth factor receptor sensitized to cisplatin by the AG1478 tyrosine kinase inhibitor. J Neurosurg 2001;95:472–9.
[24] Perera RM, Narita Y, Furnari FB, Gan HK, Murone C, Ahlkvist M, et al. Treatment of human tumor xenografts with monoclonal antibody 806 in combination with a prototypical epidermal growth factor receptor-specific antibody generates enhanced antitumor activity. Clin Cancer Res 2005;11:6390–9.
[25] Chakravarti A, Chakladar A, Delaney MA, Latham DE, Loettler JS. The epidermal growth factor receptor pathway mediates resistance to sequential administration of radiation and chemotherapy in primary human glioblastoma cells in a RAS-dependent manner. Cancer Res 2002;62:4307–15.
[26] Solomon B, Hagekyriakou J, Trivett MK, Stacker SA, McArthur GA, Cullinane C. EGFR blockade with ZD1839 (''Iressa'') potentiates the antitumour effects of single and multiple fractions of ionizing radiation in human A431 squamous cell carcinoma. Epidermal growth factor receptor. Int J Radiat Oncol Biol Phys 2003;55(3):713–23.
[27] Johnson DH, Herbst R, Giaccone G, Schiller J, Natale RB, Miller V, et al. ZD1839 (''Iressa'') in combination with paclitaxel & carboplatin in chemotherapy-naïve patients with advanced non-small-cell lung cancer (NSCLC): results from a phase III clinical trial (INTACT 2). Annals Oncol 2002;13(Suppl. 5). Abstr 4680.
[28] Lynch TJ, Bell DW, Sordella R, Gurubhagavatula S, Okimoto RA, Brannigan BW, et al. Activating mutations in the epidermal growth factor receptor underlying responsiveness of non-small-cell lung cancer to gefitinib. N Engl J Med 2004;350:2129–39.
[29] Paez JG, Jänne PA, Lee JC, Tracy S, Greulich H, Gabriel S, et al. EGFR mutations in lung cancer: correlation with clinical response to gefitinib therapy. Science 2004;304:1497–500.
[30] Levitzki A, Gazit A. Tyrosine kinase inhibition: an approach to drug development. Science (Washington DC) 1995;267:1782.
[31] Levitzki A. Protein kinase inhibitors as a therapeutic modality. Acc Chem Res 2003;36:462–9.
[32] Lichtner RB, Menrad A, Sommer A, Klar U, Schneider MR. Signaling-inactive epidermal growth factor receptor/ligand complexes in intact carcinoma cells by quinazoline tyrosine kinase inhibitors. Cancer Res 2001;61:5790–5.
[33] Osherov N, Levitzki A. Epidermal-growth-factor-dependent activation of the src-family kinases. Eur J Biochem 1994;225:1047–53.
[34] Meylan N, Grunberger T, Dadi H, Shahar M, Arpaia E, Lapidot Z, et al. Inhibition of acute lymphoblastic leukaemia by a Jak-2 inhibitor. Nature 1996;379:645–8.
[35] Partik G, Hochegger K, Schörkhuber M, Marian B. Inhibition of epidermal-growth-factor-receptor-dependent signalling by tyrphostins A25 and AG1478 blocks growth and induces apoptosis in colorectal tumour cells in vitro. J Cancer Res Clin Oncol 1999;125:379–88.
[36] Zhu XF, Liu ZC, Xie BF, Li ZM, Feng GK, Yang D, et al. EGFR tyrosine kinase inhibitor AG1478 inhibits cell proliferation and arrests cell cycle in nasopharyngeal carcinoma cells. Cancer Lett 2001;169:27–32.
[37] Nagane N, Levitzki A, Gazit A, Cavanee WK, Huang HJ. Drug resistance of human glioblastoma cells conferred by a tumour specific mutant epidermal growth factor receptor through modulation of Bcl-XL and caspase 3-like proteases. Proc Natl Acad Sci USA 1998;95:5724–9.
[38] Lei W, Mayotte EJ, Levitt LM. Enhancement of chemosensitivity and programmed cell death by tyrosine kinase inhibitors correlates with EGFR expression in non-small cell lung cancer cells. Anticancer Res 1999;19:221–8.
[39] Busse D, Doughty RS, Ramsey TT, Russell WE, Price JO, Flanagan WM, et al. Reversible G1 arrest induced by inhibition of the epidermal growth factor receptor tyrosine kinase requires up-regulation of p27KIP1 independent of MAPK activity. J Biol Chem 2000;275(10):6987–95.
[40] Johns TG, Luwor RB, Murone C, Walker F, Weinstock J, Vitali AA, et al. Antitumour efficacy of cytotoxic drugs and the monoclonal antibody 806 is enhanced by the EGF receptor inhibitor AG1478. Proc Natl Acad Sci USA 2003;100:15871–6.
[41] Sugawa N, Ekstrand AJ, James CD, Collins VP. Identical splicing of aberrant epidermal growth factor receptor transcripts from amplified rearranged genes in human glioblastomas. Proc Natl Acad Sci USA 1990;87:8602–6.
[42] Okimoto K, Rajewski RA, Uekama K, Jona JA, Stella VJ. The interaction of charged and uncharged drugs with neutral (HP-β-CD) and anionically charged (SBE7-β-CD) beta-cyclodextrins. Pharm Res 1996;13(2):256–64.
[43] Ueda H, Ou D, Endo T, Nagase H, Tomono K, Nagai T. Evaluation of a sulfobutyl ether beta-cyclodextrin as a solubilizing/stabilizing agent for several drugs. Drug Dev Ind Pharm 1998;24(9):863–7.
[44] Loftsson T, Brewster ME. Pharmaceutical applications of cyclodextrins. I. Drug solubilization and stabilization. J Pharm Sci 1996;85:1017–27.
[45] Davis ME, Brewster ME. Cyclodextrin-based pharmaceutics: past, present and future. Nat Rev Drug Discov 2004;3:10235.
[46] Walker F, Hibbs ML, Zhang HH, Gonez LJ, Burgess AW. Biochemical characterization of mutant EGF receptors expressed in the hemopoietic cell line BaF/3. Growth Factors 1998;16:53–67.
[47] Whitehead RH, Macrae FA, St John DJ, Ma J. A colon cancer cell line (LIM1215) derived from a patient with inherited nonpolyposis colorectal cancer. J Natl Cancer Inst 1985;74:759–65.
[48] Ellis AG, Nice EC, Weinstock J, Levitzki A, Burgess AW, Webster LK. High-performance liquid chromatographic analysis of the tyrphostin AG1478, a specific inhibitor of the epidermal growth factor receptor tyrosine kinase, in mouse plasma. J Chromatogr B 2001;754:193–9.
[49] Waynforth HB, Flecknell PA. Experimental and surgical technique in the rat, 2nd ed., London: Academic press Ltd.; 1994.
[50] Jungbluth AA, Stockert E, Huang HJ, Collins VP, Coplan K, Iversen K, et al. A monoclonal antibody recognizing human cancers with amplification/overexpression of the human epidermal growth factor receptor. Proc Natl Acad Sci USA 2003;100:639–44.
[51] McConnell HM, Owicki JC, Parce JW, Miller DL, Baxter GT, Wada HG, et al. The cytosensor microphysiometer: biological applications of silicon technology. Science 1992;257:1906–12.
[52] Lui KE, Panchal AS, Santhanagopal A, Dixon SJ, Bernier SM. Epidermal growth factor stimulates proton efflux from chondrocytic cells. J Cell Physiol 2002;192:102–12.
[53] Lauffenburger DA, Oehrtman GT, Walker L, Wiley HS. Real-time quantitative measurement of autocrine ligand binding indicates that autocrine loops are spatially localized. Proc Natl Acad Sci USA 1998;95:15368–73.
[54] Owicki JC, Parce JW, Kercso KM, Sigal GB, Muir VC, Venter JC, et al. Continuous monitoring of receptor-mediated changes in the metabolic rates of living cells. Proc Natl Acad Sci USA 1990;87:4007–11.

[55] Chan SD, Antoniucci DM, Fok KS, Alajoki ML, Harkins RN, Thompson SA, et al. Heregulin activation of extracellular acidification in mammary carcinoma cells is associated with expression of HER2 and HER3. J Biol Chem 1995;270:22608–13.
[56] Walker F, Orchard SG, Jorissen RN, Hall NE, Zhang HH, Hoyne PA, et al. CR1/CR2 interactions modulate the functions of the cell surface epidermal growth factor receptor. J Biol Chem 2004;279:22387–98.
[57] Smith ER, Hadidian Z, Mason MM. The single- and repeated-dose toxicity of dimethylsulfoxide. Ann NY Acad Sci 1967;141:96–109.
[58] McKillop D, Partridge EA, Kemp JV, Spence MP, Kendrew J, Barnett S, et al. Tumor penetration of gefitinib (Iressa), an epidermal growth factor receptor tyrosine kinase inhibitor. Mol Cancer Ther 2005;4(4):641–9.
[59] Fredriksson A, Johnstrom P, Thorell JO, von Heijne G, Hassan M, Eksborg S, et al. In vivo evaluation of the biodistribution of 11C-labeled PD153035 in rats without and with neuroblastoma implants. Life Sci 1999;65:165–74.
[60] Siegel-Lakhai WS, Beijnen JH, Schellens JHM. Current knowledge and future directions of the selective epidermal growth factor receptor inhibitors erlotinib (Tarceva®) and gefitinib (Iressa®). Oncologist 2005;10:579–89.
[61] Twombly R. Failing survival advantage in crucial trial, future of Iressa in jeopardy. J Natl Cancer Inst 2005;97:249–50.
[62] Fuster LM, Sandler AB. Select clinical trials of erlotinib (OSI-774) in non-small-cell lung cancer with emphasis on phase III outcomes. Clin Lung Cancer 2004;6(Suppl. 1):S24–9.